This is the peer-reviewed, final accepted version for American Mineralogist, published by the Mineralogical Society of America.
The published version is subject to change. Cite as Authors (Year) Title. American Mineralogist, in press.
DOI: https://doi.org/10.2138/am-2022-8335. http://www.minsocam.org/

Revision #1

Pomite and pseudopomite, two new carbonate-encapsulating mixed-valence polyoxovanadate minerals

ANTHONY R. KAMPF[1ξ], JOHN M. HUGHES[2], CHI MA[3], JOE MARTY[1], AND TIMOTHY P. ROSE[4]

[1] Mineral Sciences Department, Natural History Museum of Los Angeles County, 900 Exposition Boulevard, Los Angeles, CA 90007, U.S.A.
[2] Department of Geology, University of Vermont, Burlington, VT 05405, U.S.A.
[3] Division of Geological and Planetary Sciences, California Institute of Technology, Pasadena, CA 91125, U.S.A.
[4] Nuclear and Chemical Sciences Division, Lawrence Livermore National Laboratory, Livermore, CA 94550, U.S.A.

ABSTRACT

Pomite (IMA2021-063), ideally $Ca_3[V^{4+}_5V^{5+}_{10}O_{37}(CO_3)]\cdot 37H_2O$, and pseudopomite (IMA2021-064), ideally $Ca_{3.5}[V^{4+}_6V^{5+}_9O_{37}(CO_3)]\cdot 32H_2O$, are two new polyoxometalate minerals from the Blue Streak mine, Bull Canyon, Montrose County, Colorado, U.S.A. Pomite properties: striated blades up to ~1 mm long; very dark green-blue color; green-blue streak; vitreous luster; brittle; Mohs hardness ≈ 2; irregular, splintery fracture; good cleavages on {010} and {001}; 2.19(2) g cm^{-3} density; refractive indices in the vicinity of 1.70; weakly birefringent with little or no pleochroism. Pseudopomite properties: striated prisms and blades up to ~1 mm; very dark blue-green color; blue-green streak; vitreous luster; brittle; Mohs hardness ≈ 2; curved, irregular fracture; probably two fair cleavages, {100} and {001}; 2.40(2) g cm^{-3} density; refractive indices in the vicinity of 1.72; no discernable birefringence or pleochroism. Electron microprobe

ξ Email: akampf@nhm.org

analyses provided the empirical formulas $Ca_{3.11}[V^{4+}_{5.23}V^{5+}_{9.77}O_{37}(CO_3)]\cdot 37H_2O$ and $Ca_{3.49}[V^{4+}_{5.98}V^{5+}_{9.02}O_{37}(CO_3)]\cdot 29H_2O$ for pomite and pseudopomite, respectively. Pomite is triclinic, *P*-1, with a = 12.3668(10), b = 12.9692(12), c = 22.068(2) Å, α = 99.038(7), β = 95.689(7), γ = 103.249(7)°, V = 3368.7(5) Å^3, and Z = 2. Pseudopomite is triclinic, *P*-1, with a = 12.2910(18), b = 12.6205(15), c = 20.917(3) Å, α = 77.381(6), β = 85.965(5), γ = 64.367(7)°, V = 2853.6(7) Å^3, Z = 2. The crystal structures of both minerals (pomite, R_1 = 0.103; pseudopomite, R_1 = 0.116) contain a novel $[V^{4+}_{x}V^{5+}_{15-x}O_{37}(CO_3)]^{(1+x)-}$ heteropolyanion, which is unique in natural and synthetic materials but has similarities to the $[V^{4+}_{8}V^{5+}_{7}O_{36}(CO_3)]^{7-}$ and $[H_8V^{4+}_{15}O_{36}(CO_3)]^{6-}$ heteropolyanions reported in synthetic phases.

Keywords: pomite; pseudopomite; new mineral; crystal structure; polyoxometalate; vanadate; carbonate encapsulation; Blue Streak mine, Montrose County, Colorado, U.S.A.

Introduction

The Uravan mineral belt along the eastern edge of the Colorado Plateau has long been recognized as a unique environment for uranium and vanadium minerals. In the 1950s, in conjunction with the national effort led by the U.S. Geological Survey (USGS) and Atomic Energy Commission (AEC), an intensive program of study was undertaken on the vanadium ores of the region, led largely by H.T. Evans, Jr., of the USGS. The innumerable mines in the Uravan belt have exploited uranium and vanadium ores in roll-front deposits in the sandstone of the Salt Wash member of the Morrison Formation (Carter and Guiltieri 1965; Shawe 2011) and have provided a rich environment for the study of vanadium mineralogy under ambient temperatures and a variety of Eh and pH conditions.

Following the initial USGS investigations of the 1950s, the mineralogy of the Uravan deposits received little attention until recently when collecting efforts, organized primarily by one of the authors (JM), have yielded extensive suites of secondary U and V minerals from the increasingly limited number of mines that are still accessible. Investigations have led to the discovery of more than 30 new minerals; the new mineral descriptions and attendant crystal structure solutions have significantly enhanced our knowledge on the mineralogy of vanadium. Of particular interest in these studies is the discovery and description of many new minerals that are in a chemical class known as *polyoxometalates* (often abbreviated as POMs), a type of compound with many technological and medical applications that have been extensively studied by chemists and material scientists (Kampf et al. 2019). Polyoxometalates are clusters of three or more transition-metal-centered polyhedra that are linked by sharing oxygen ligands between and among the polyhedra. The clusters are usually anionic in charge and are linked to form closed (isolated) three-dimensional frameworks.

In a detailed summary of polyoxometalate minerals, Krivovichev (2020) observed that 34 of the 42 naturally known (at that writing) POM complexes have been discovered in the 21st century, and he noted that the vast majority of POM minerals are polyoxovanadates (POVs). All of the 30 known POV minerals are found in the Uravan mineral belt and all but two of these were first discovered there. Twenty-one of these POV minerals contain the decavanadate isopolyanion, $[V_{10}O_{28}]^{6-}$, formed of ten VO_6 octahedra linked through corner- and edge-sharing. These comprise the pascoite mineral family (Kampf et al. 2021). The other POV minerals (followed by their POV clusters in brackets) are sherwoodite $[AlV^{4+}{}_2V^{5+}{}_{12}O_{40}]^{9-}$ (Evans and Konnert 1978), the five members of the vanarsite family $[(V^{4+}{}_xV^{5+}{}_{10-x})O_{28}]^{(6+x)-}$ (Kampf et al.

2016, 2020), kegginite $[As^{5+}V^{5+}_{12}O_{40}(VO)]^{12-}$ (Kampf et al. 2017), bicapite $[H_2PV_{12}O_{40}(VO)_2]^{7-}$ (Kampf et al. 2019), and, reported herein, pomite and pseudopomite $[V^{4+}_{x}V^{5+}_{15-x}O_{37}(CO_3)]^{(1+x)-}$.

The new minerals and their names were approved by the Commission on New Minerals, Nomenclature and Classification of the International Mineralogical Association (IMA2021–063, pomite; IMA2021-064, pseudopomite). The name "pomite" is based on the acronym POM, which stands for polyoxometalate. Initially, the two minerals were thought to be a single phase because of their similar appearances and compositions, as well as their intimate association. The second phase, named "pseudopomite" for obvious reasons, was recognized only when its powder diffraction pattern could not be matched to the pattern calculated from the structure of pomite. The holotype specimen containing both pomite and pseudopomite is deposited in the collections of the Natural History Museum of Los Angeles County, Los Angeles, California, USA, under catalogue number 76155.

OCCURRENCE

Pomite and pseudopomite were discovered underground in the Blue Streak mine, Bull Canyon, Montrose County, Colorado, USA (38.199434 -108.839946), about 13 km west of the town of Naturita. The minerals were collected in April, 2019 by one of the authors (TPR), and have been found very sparingly on only several small specimens. They occur on montroseite-corvusite-bearing sandstone in close association with calcite. Interestingly, Evans and Garrels (1957) recognized such an environment in their landmark work, noting that "two distinct branches appear in the alteration sequence (of primary montroseite): one is confined to acid conditions characteristic of zones of primary vanadium oxide concentration in the sandstone in the presence of pyrite; and the other occurs in more basic conditions where calcite is common".

Pomite and pseudopomite occur in the latter, calcite-present, alteration sequence.

The Blue Streak mine is in the Uravan mineral belt, in which uranium and vanadium minerals occur together in bedded or roll-front deposits in the sandstone of the Salt Wash member of the Jurassic Morrison formation (Carter and Gualtieri, 1965; Shawe, 2011). The new minerals form from the oxidation of montroseite-corvusite assemblages in a moist environment. Mining operations have exposed unoxidized and oxidized phases. Under ambient temperatures and generally oxidizing near-surface conditions, water reacts with pyrite to form aqueous solutions with relatively low pH. The various secondary vanadate phases that form depend upon prevailing Eh-pH conditions (Evans and Garrels 1957) and the presence of other cations.

APPEARANCE, OPTICAL PROPERTIES AND PHYSICAL PROPERTIES

Both pomite and pseudopomite crystals are very dark green blue, appearing black. Pomite crystals are striated blades up to about 1 mm long (Figs. 1 and 2), whereas pseudopomite crystals are striated prisms and blades up to about 1 mm long (Figs. 3 and 4). Both minerals display blue-green streak and vitreous luster, and are transparent (only on very thin edges). The minerals display a brittle tenacity, are non-fluorescent, have a Mohs hardness ~2, and have no observed parting. Pomite displays good {010} and {001} cleavages; pseudopomite probably has two fair cleavages, {100} and {001}; however, the fragility of crystals makes it difficult to determine the cleavage directions with certainty. For pomite, the fracture is irregular and splintery; for pseudopomite, the fracture is curved and irregular. The densities for pomite and pseudopomite were measured as 2.19(2) g/cm^3 and 2.40(2) g/cm^3, respectively, both by floatation in methylene iodide – toluene. For pomite, the calculated density is 2.176 g/cm^3 for the empirical formula and 2.171 g/cm^3 for the ideal formula; for pseudopomite, the calculated density is 2.419 g/cm^3 for

both the empirical and ideal formulas.

Pomite and pseudopomite crystals are very difficult to examine optically because of their dark color. For pomite, thin fragments are only weakly birefrigent and exhibit very little, if any, pleochroism. All three indices of refraction appear to be in the vicinity of 1.70, and the Gladstone-Dale relation predicts an average index of refraction of 1.675 calculated on the basis of the empirical formula. For pseudopomite, all three indices of refraction appear to be in the vicinity of 1.72, and the Gladstone-Dale relation predicts an average index of refraction of 1.736 calculated on the basis of the empirical formula.

CHEMISTRY OF POMITE AND PSEUDOPOMITE

Analyses of pomite (11 points on two crystals) and pseudopomite (10 points on two crystals) were performed at Caltech on a JEOL 8200 electron microprobe in WDS mode. Analytical conditions were 15 kV accelerating voltage, 5 nA beam current and 2 μm beam diameter. H_2O and CO_2 were not determined directly because of extreme paucity of material. For pomite, the H_2O and CO_2 contents were calculated by stoichiometry on the basis of 15 V and 77 O *apfu* as indicated by the crystal structure refinement. Note that the interstitial portion of the pomite structure exhibits considerable disorder. Note that the structure refinement provided 76.19 O *apfu*, but significant unresolved electron density led us to round up the O content to 77 *apfu*, which we use for the ideal formula. For pseudopomite, the H_2O and CO_2 contents were calculated by stoichiometry on the basis of 15 V and 69 O *apfu* as indicated by the crystal structure refinement.

Table 1 contains the chemical analytical data for pomite and pseudopomite. For pomite, the empirical formula (based on O = 77 *apfu*) is $Ca_{3.11}[V^{4+}_{5.23}V^{5+}_{9.77}O_{37}(CO_3)]\cdot 37H_2O$, the

simplified formula is $Ca_{3+x}[V^{4+}_{5+2x}V^{5+}_{10-2x}O_{37}(CO_3)]\cdot 37H_2O$ ($x \approx 0 - 0.20$), and the ideal formula is $Ca_3[V^{4+}_5V^{5+}_{10}O_{37}(CO_3)]\cdot 37H_2O$, which requires CaO 7.64, VO_2 18.83, V_2O_5 41.28, CO_2 2.00, H_2O 30.26. For pseudopomite, the empirical formula (based on O = 69 *apfu*) is $Ca_{3.49}[V^{4+}_{5.98}V^{5+}_{9.02}O_{37}(CO_3)]\cdot 29H_2O$, the simplified formula is $Ca_{3.5}[V^{4+}_6V^{5+}_9O_{37}(CO_3)]\cdot 29H_2O$, and the ideal formula is $Ca_{3.5}[V^{4+}_6V^{5+}_9O_{37}(CO_3)]\cdot 32H_2O$, which requires CaO 9.44, VO_2 23.94, V_2O_5 39.37, CO_2 2.12, H_2O 25.13.

THE ATOMIC ARRANGEMENTS OF POMITE AND PSEUDOPOMITE

Experimental

X-ray powder diffraction data were recorded using a Rigaku R-Axis Rapid II curved imaging plate microdiffractometer with monochromatized Mo*K*α radiation. A Gandolfi-like motion on the φ and ω axes was used to randomize the sample. The pattern obtained was a good fit for that calculated from the structure. The patterns of both structures are dominated by two low-angle peaks, one of which is a composite of numerous lines, and all other peaks are relatively indistinct composites of numerous low-intensity lines. Observed *d* values and intensities were derived by profile fitting using JADE Pro software (Materials Data, Inc.). Complete powder diffraction results are on deposit[1].

Single-crystal X-ray studies were carried out using the same instrument, and gave the following data. Pomite: Crystal System: Triclinic, *P*-1 (#2), a = 12.3668(10), b = 12.9692(12), c = 22.068(2) Å, α = 99.038(7), β = 95.689(7), γ = 103.249(7)°, V = 3368.7(5) Å^3, and Z = 2. Pseudopomite: Triclinic, *P*-1 (#2), a = 12.2910(18), b = 12.6205(15), c = 20.917(3) Å,

This is the peer-reviewed, final accepted version for American Mineralogist, published by the Mineralogical Society of America.
The published version is subject to change. Cite as Authors (Year) Title. American Mineralogist, in press.
DOI: https://doi.org/10.2138/am-2022-8335. http://www.minsocam.org/

160 $\alpha = 77.381(6)$, $\beta = 85.965(5)$, $\gamma = 64.367(7)°$, $V = 2853.6(7)$ Å^3, $Z = 2$. Complete details of data
161 collection are provided in deposited CIFs for each phase.[1]

162 The Rigaku CrystalClear software package was used for processing the structure data,
163 including the application of an empirical absorption correction using the multi-scan method with
164 ABSCOR (Higashi 2001). The structures were solved using SHELXT (Sheldrick 2015a).
165 SHELXL-2016 (Sheldrick 2015b) was used for the refinement of the structures. For pomite, the
166 structural unit is well ordered except for the V15 site, which is split into two sites, V15A and
167 V15B, separated by 1.55 Å. These sites were jointly refined to $V15A_{0.838}V15B_{0.162(8)}$. The V15A
168 site has tetrahedral coordination and the V15B site has square-pyramidal five-fold coordination,
169 discussed subsequently. The interstitial complex, which includes Ca and H_2O sites, exhibits
170 significant disorder and includes three fully occupied Ca sites, two low-occupancy Ca sites, 31
171 fully occupied H_2O sites and nine partially occupied H_2O sites. Many of the H_2O sites exhibit
172 large displacement parameters. Not surprisingly, difference-Fourier syntheses failed to locate any
173 H atom positions. The final R_1 is 0.103.

174 For pseudopomite, the structural unit is well ordered. The interstitial complex, which
175 includes Ca and H_2O sites, exhibits significant disorder and includes three fully occupied Ca
176 sites, one approximately half-occupied Ca site, 27 fully occupied H_2O sites and three adjacent
177 partially occupied H_2O sites (with a total occupancy set to 2.0). Many of the H_2O sites exhibit
178 large displacement parameters and prolate or oblate ellipsoids. As in pomite, difference-Fourier
179 syntheses failed to locate any H atom positions. The final R_1 is 0.116.

[1] Deposit item AMS-22-xx1-4 for complete powder diffraction patterns and Crystallographic Information Files. Deposit items are available two ways: for paper copies, contact the Business Office of the Mineralogical Society of America (see inside front cover of recent issue) for price information. For an electronic copy, visit the MSA web site at http://www.minsocam.org, go to the *American Mineralogist* Contents, find the table of contents for the specific volume/issue wanted, and then click on the deposit link there.

Data collection and refinement details are given in the deposited CIFs, as are atom coordinates and displacement parameters; note that the crystals were not strong diffractors, yielding sin θ/λ values of 0.50 and 0.53 for the two crystals. Selected bond distances and bond-valence sums (BVS) for pomite are reported in Table 2 and those for pseudopomite in Table 3.

The Structural Unit in Pomite and Pseudopomite

The structures of pomite and pseudopomite consist of two distinct parts, a structural unit and an interstitial complex, as suggested by Schindler and Hawthorne (2001) for such hydrated minerals with a polyanion. Figure 5 displays the structural unit found in both new phases compared with the heteropolyanion found in synthetic phases described below. Figure 6 illustrates the two atomic arrangements, displaying the disposition of the structural unit and interstitial units in pomite and pseudopomite.

The $[V^{4+}_{5}V^{5+}_{10}O_{37}(CO_3)]^{6-}$ heteropolyanion forming the structural unit in pomite and the essentially identical $[V^{4+}_{6}V^{5+}_{9}O_{37}(CO_3)]^{7-}$ heteropolyanion forming the pseudopomite structural unit are comprised of a cluster of nine VO_6 octahedra, five VO_5 square-based pyramids (ignoring the small amount of V contained in the V15B site in pomite), one VO_4 tetrahedron, and a planar carbonate CO_3 group. The VO_6 and VO_5 polyhedra link to one another by sharing edges and corners; the VO_4 tetrahedron links to the other vanadate polyhedra by sharing two of its corners; the carbonate group, is located at the center of the cluster, sharing its three corners with VO_6 octahedra. This heteropolyanion is unique among natural and synthetic materials, but is very similar to the $[V^{4+}_{8}V^{5+}_{7}O_{36}(CO_3)]^{7-}$ heteropolyanion reported by Müller et al. (1990) and Yamase and Ohtaka (1994) and the $[H_8V^{4+}_{15}O_{36}(CO_3)]^{6-}$ heteropolyanion reported by Mulkapuri et al. (2019). The heteropolyanion in pomite and pseudopomite differs from the aforementioned

synthetic heteropolyanions only in having a VO_4 tetrahedron in place of one VO_5 square pyramid (V15; Figs. 5 and 6). However, it should be noted that this $V15O_4$ tetrahedron in pomite is only 0.838 occupied. The complementary 0.162-occupied V15B site 1.55 Å from the V15A site is located at the center of the "missing" VO_5 square pyramid observed in the aforementioned synthetic phases (Figure 5). The fact that the V15 polyhedra are split in pomite can be attributed to the valence of the V ions at that site. In pseudopomite, all the V15 exists as V^{5+}, and occupies the V15 tetrahedron, with a bond-valence sum on V15 of 5.32 vu. In pomite, V15 is mixed-valent V^{4+}/V^{5+}. The V^{5+} (0.838/1.00) occupies the V15A tetrahedron, and has an appropriate bond-valence sum of 5.07 vu. However, the small proportion of V^{4+} (0.162/1.00) would have a bond-valence sum of 4.81 in that site, dramatically overbonded, and V^{4+} does not occur in tetrahedral coordination (Schindler et al. 2000). Thus, the V^{4+} in site V15 splits to the V15B site, a square-based pyramid similar to that in $[Na_6(H_2O)_{24}]$ $[H_8V^{4+}{}_{15}O_{36}(CO_3)]$ $\cdot 3N_2H_4 \cdot 10H_2O$ (Mulkapuri et al. 2019). The bond-valence sum of V^{4+} in that site is 3.78 vu. Thus, the V15 site splits to sites appropriate for V^{5+} (the V15A tetrahedron) and V^{4+} (the V15B square-based pyramid).

The Interstitial Units in Pomite and Pseudopomite

Pomite. Balancing the charge of the anionic heteropolyanions in each of the two new minerals are the interstitial complexes, which also serve to link the individual structural units. In pomite, with ideal formula $Ca_3[V^{4+}{}_5V^{5+}{}_{10}O_{37}(CO_3)]\cdot 37H_2O$, the interstitial unit has a composition of $[Ca_3 \cdot 37H_2O]^{6+}$.

The interstitial complex in pomite includes three fully occupied Ca sites (Ca1, Ca2 and

Ca3) and two low-occupancy Ca sites (Ca4 and Ca5). The total refined occupancy of the Ca sites is 3.20 *apfu*, a bit higher than the 3.11 Ca *apfu* based on the EPMA, although it should be noted that the Ca4 and Ca5 sites are only 2.65 Å apart, indicating that they are probably partially occupied by the O atoms of H_2O groups, i.e., when an H_2O group is located at Ca4, it is coordinated to the Ca at Ca5, and vice versa. The excess Ca above 3 *apfu* is easily charge balanced by varying the relative amounts of 4+ and 5+ V. To allow for this, the formula can be expressed as $Ca_{3+x}[V^{4+}_{5+2x}V^{5+}_{10-2x}O_{37}(CO_3)]\cdot 37H_2O$ ($x \approx 0 - 0.20$), whereas the ideal formula, $Ca_3[V^{4+}_5V^{5+}_{10}O_{38}(CO_3)]\cdot 37H_2O$, corresponds to $x = 0$.

Ca1 and Ca3 are coordinated to two peripheral O sites of the heteropolyanion and to six H_2O groups in the interstitial complex. Ca2 is coordinated to one peripheral O site of the heteropolyanion and to seven H_2O groups. Ca4 is coordinated eight H_2O sites, two of which are located at Ca5. Ca5 coordinates to one peripheral O site of the heteropolyanion and to seven H_2O groups, one of which are located at Ca4. The complete structure, combining the structural unit and the interstitial complex, is shown in Figure 6.

Pseudopomite. The interstitial complex includes three fully occupied Ca sites (Ca1, Ca2 and Ca3) and one approximately half-occupied Ca site (Ca4). The total refined occupancy of the Ca sites is 3.54 *apfu*, very close to the 3.49 Ca *apfu* based on the EPMA. Ca1 coordinates to two peripheral O sites of the heteropolyanion and to six H_2O groups in the interstitial complex. Ca2 is coordinated to two peripheral O sites of the heteropolyanion and to seven H_2O groups. Ca3 is coordinated to three peripheral O sites of the heteropolyanion and to five H_2O groups. Ca4 is coordinated to two peripheral O sites of the heteropolyanion and to six H_2O groups. The BVS for Ca3 (1.64 *vu*) is significantly low and that for Ca4 (2.47 *vu*) is significantly high; however, as noted above, many of the H_2O sites exhibit large displacement parameters and prolate or oblate

ellipsoids, indicating disorder in the interstitial complex, which certainly impacts the reliability of the BVS values for the Ca sites. The complete structure is shown in Figure 6.

IMPLICATIONS

Krivovichev (2020), in his survey of polyoxometalate minerals, made the important observation that the discovery of POM minerals is one of the specific landmarks of descriptive mineralogy and mineralogical crystallography of our time. The most recently discovered POM minerals, pomite and pseudopomite are the first to incorporate carbonate as the central heteropolyhedral group of the POM. Synthetic carbonate-bearing POMs have been suggested as useful for the capture of atmospheric carbon. For example, Mulkapuri et al. (2019) synthesized a vanadium POM with a structural unit of $[H_8V^{IV}_{15}O_{36}(CO_3)^{6-}]$. During the synthesis, CO_2 was not used as a reactant; the source of the carbonate was absorbed aerial CO_2 in the pertinent aqueous alkaline reaction, suggesting that the POM can be used to sequester atmospheric CO_2. The use of polyoxometalates as a means of CO_2 fixation is a fruitful area of future research (Yu et al. 2018), and naturally occurring phases, such as pomite and pseudopomite, may prove to be important guides in that respect.

Acknowledgments

Reviewers Michael Schindler, two anonymous reviewers, and Associate Editor Diego Gatta are sincerely thanked for constructive comments, which improved the manuscript. This study was funded, in part, by the John Jago Trelawney Endowment to the Mineral Sciences Department of the Natural History Museum of Los Angeles County.

272

273

REFERENCES CITED

Burns, P.C. (2020) Complex minerals preserve natural geochemically important nanoscale metal oxide clusters. Acta Crystallographica, B76, 512–513.

Brown, I.D. and Altermatt, D. (1985) Bond-valence parameters obtained from a systematic analysis of the Inorganic Crystal Structure Database. Acta Crystallographica, B41, 244–247.

Carter, W.D., and Gualtieri, J.L. (1965) Geology and uranium–vanadium deposits of the La Sal quadrangle, San Juan County, Utah, and Montrose County, Colorado. U.S. Geological Survey Professional Paper 508.

Cooper, M.A., Hawthorne, F.C., Kampf, A.R., and Hughes, J.M. (2019) Determination of V^{4+}:V^{5+} ratios in the $[V_{10}O_{28}]$ decavanadate polyanion. The Canadian Mineralogist, 57(2), 235-244.

Evans, H.T., Jr., and Garrels, R.M. (1957) Thermodynamic equilibria of vanadium in aqueous systems as applied to the interpretation of the Colorado Plateau ore deposits. Trace Elements Investigation Report 666, United States Department of the Interior, U.S. Geological Survey.

Higashi, T. (2001) ABSCOR. Rigaku Corporation, Tokyo.

Kampf, A.R., Hughes, J.M., Nash, B.P., and Marty, J. (2016) Vanarsite, packratite, morrisonite, and gatewayite: four new minerals containing the $[As^{3+}V^{4+,5+}{}_{12}As^{5+}{}_{6}O_{51}]$ heteropolyanion, a novel polyoxometalate cluster. The Canadian Mineralogist, 54, 145-162.

Kampf, A.R., Hughes, J.M., Nash, B.P., and Marty, J. (2017) Kegginite, $Pb_3Ca_3[AsV_{12}O_{40}(VO)]\cdot 20H_2O$, a new mineral with an ε-isomer of the Keggin anion. American Mineralogist, 102, 461-465.

Kampf, A.R., Hughes, J.M., Nash, B.P., and Marty, J. (2019) Bicapite, $KNa_2Mg_2(H_2PV^{5+}_{14}O_{42})\cdot 25H_2O$, a new mineral with a bicapped Keggin anion from the Pickett Corral mine, Montrose County, Colorado, USA. American Mineralogist, 104, 1851-1856.

Kampf, A.R., Hughes, J.M., Nash, B.P., Marty, J., and Rose, T.P. (2020) Lumsdenite, $NaCa_3Mg_2(As^{3+}V^{4+}_2V^{5+}_{10}As^{5+}_6O_{51})\cdot 45H_2O$, a new polyoxometalate mineral from the Packrat mine, Mesa County, Colorado, USA. The Canadian Mineralogist, 58, 137-151.

Kampf, A.R., Hughes, J.M., Cooper, M.A., Hawthorne, F.C., Nash, B.P., Olds, T.A., Adams, P.M. and Marty, J. (2021) The pascoite family of minerals, including the redefinition of rakovanite. The Canadian Mineralogist, 59, 771-779.

Krivovichev, S. V. (2020). Polyoxometalate clusters in minerals: review and complexity analysis. Acta Crystallographica, B76, 618–629.

Mulkapuri, S., Kurapati, S.K., and Das, S.K. (2019) Carbonate encapsulation from dissolved atmospheric CO_2 into a polyoxovanadate capsule. Dalton Transactions, 48, 8773-8781.

Müller, A., Penk, M., Rohlfing, R., Krickemeyer, E. and Döring, J. (1990) Topologically Interesting Cages for Negative Ions with Extremely High "Coordination Number": An Unusual Property of V-O Clusters. Angewandte Chemie International Edition in English, 29, 926–927.

316 Schindler, M. and Hawthorne, F.C. (2000) A bond-valence approach to the structure, chemistry,
317 and paragenesis of hydroxyl-hydrated oxysalt minerals. I. Theory. The Canadian
318 Mineralogist, 39, 1225–1242.
319 Schindler, M., Hawthorne, F.C., and Baur, W.H. (2000) Crystal chemical aspects of vanadium:
320 polyhedral geometries, characteristic bond valences, and polymerization of (VOn) polyhedra.
321 Chemistry of Materials, 12, 1248-1259.
322 Shawe, D.R. (2011) Uranium-vanadium deposits of the Slick Rock district, Colorado. U.S.
323 Geological Survey Professional Paper 576-F.
324 Sheldrick, G.M. (2015a) SHELXT – Integrated space-group and crystal-structure determination.
325 Acta Crystallographica, A71, 3–8.
326 Sheldrick, G.M. (2015b) Crystal Structure refinement with SHELX. Acta Crystallographica,
327 C71, 3–8.
328 Yamase, T. and Ohtaka, K. (1994) Photochemistry of polyoxovanadates. Part 1. Formation of the
329 anion-encapsulated polyoxovanadate $[V_{15}O_{36}(CO_3)]^{7-}$ and electron-spin polarization of α-
330 hydroxyalkyl radicals in the presence of alcohols. Journal of the Chemical Society, Dalton
331 Transactions, 18, 2599–2608.
332 Yu, B., Zou, B., and Hu, C.-W. (2018) Recent applications of polyoxometalates in CO_2 capture
333 and transformation. Journal of CO_2 Utilization, 26, 314-322.
334

This is the peer-reviewed, final accepted version for American Mineralogist, published by the Mineralogical Society of America.
The published version is subject to change. Cite as Authors (Year) Title. American Mineralogist, in press.
DOI: https://doi.org/10.2138/am-2022-8335. http://www.minsocam.org/

FIGURE 1. Pomite crystals; the field of view is 0.84 mm across.

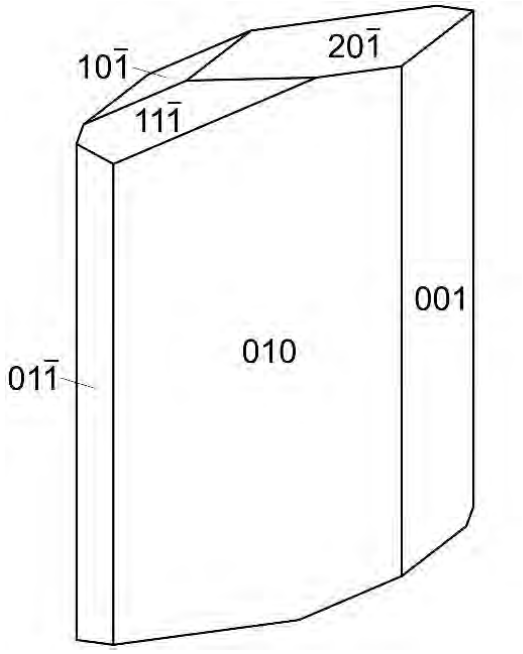

FIGURE 2. Crystal drawing of pomite, clinographic projection in non-standard orientation, **a** vertical.

This is the peer-reviewed, final accepted version for American Mineralogist, published by the Mineralogical Society of America.
The published version is subject to change. Cite as Authors (Year) Title. American Mineralogist, in press.
DOI: https://doi.org/10.2138/am-2022-8335. http://www.minsocam.org/

FIGURE 3. Pseudopomite crystals; the field of view is 1.7 mm across.

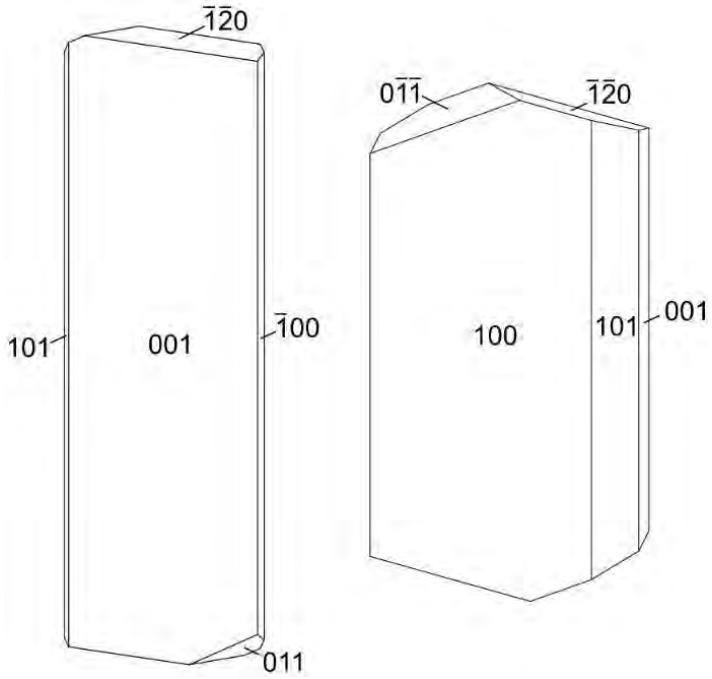

FIGURE 4. Crystal drawings of two blade habits of pseudopomite, clinographic projections in non-standard orientations, **b** vertical.

This is the peer-reviewed, final accepted version for American Mineralogist, published by the Mineralogical Society of America.
The published version is subject to change. Cite as Authors (Year) Title. American Mineralogist, in press.
DOI: https://doi.org/10.2138/am-2022-8335. http://www.minsocam.org/

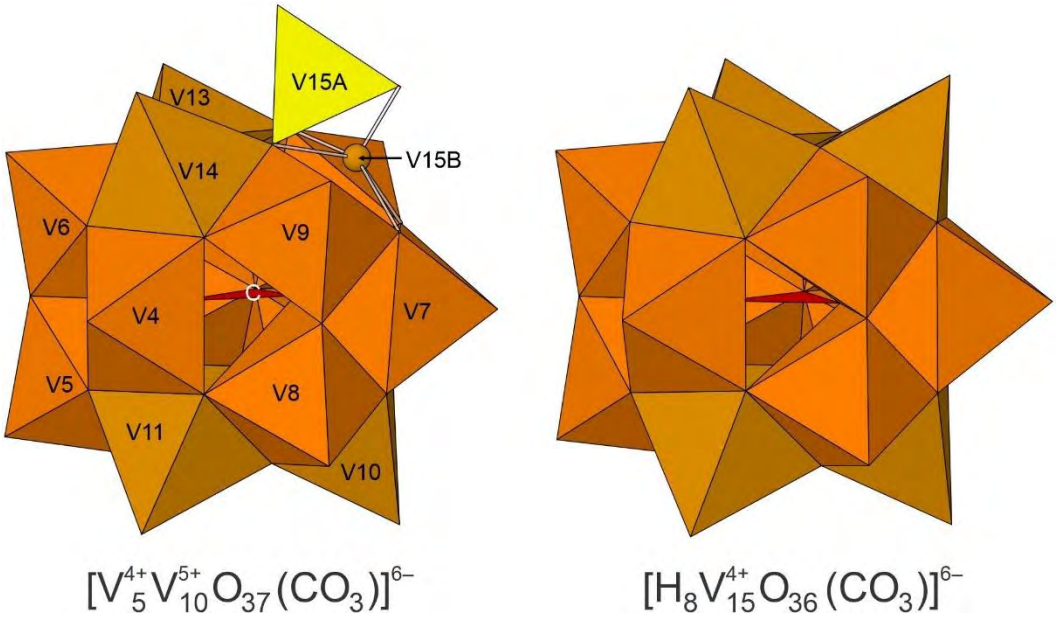

FIGURE 5. Heteropolyanions in pomite (left, with ideal formula of heteropolyanion) and $[Na_6(H_2O)_{24}]$ $[H_8V^{4+}{}_{15}O_{36}(CO_3)]\cdot 3N_2H_4\cdot 10H_2O$ (right) (Mulkapuri *et al*., 2019). The VO_6 octahedra are orange, the VO_5 square pyramids are light brown, the VO_4 tetrahedron is yellow and the central CO_3 triangles are red. The low-occupancy V15B site is shown as a light brown ball with VO_5 square pyramidal bonds shown as white sticks. The topology of the heteropolyhedron in pseudopomite is identical to that in pomite except that the low-occupancy V15B site is completely vacant in pseudopomite.

This is the peer-reviewed, final accepted version for American Mineralogist, published by the Mineralogical Society of America.
The published version is subject to change. Cite as Authors (Year) Title. American Mineralogist, in press.
DOI: https://doi.org/10.2138/am-2022-8335. http://www.minsocam.org/

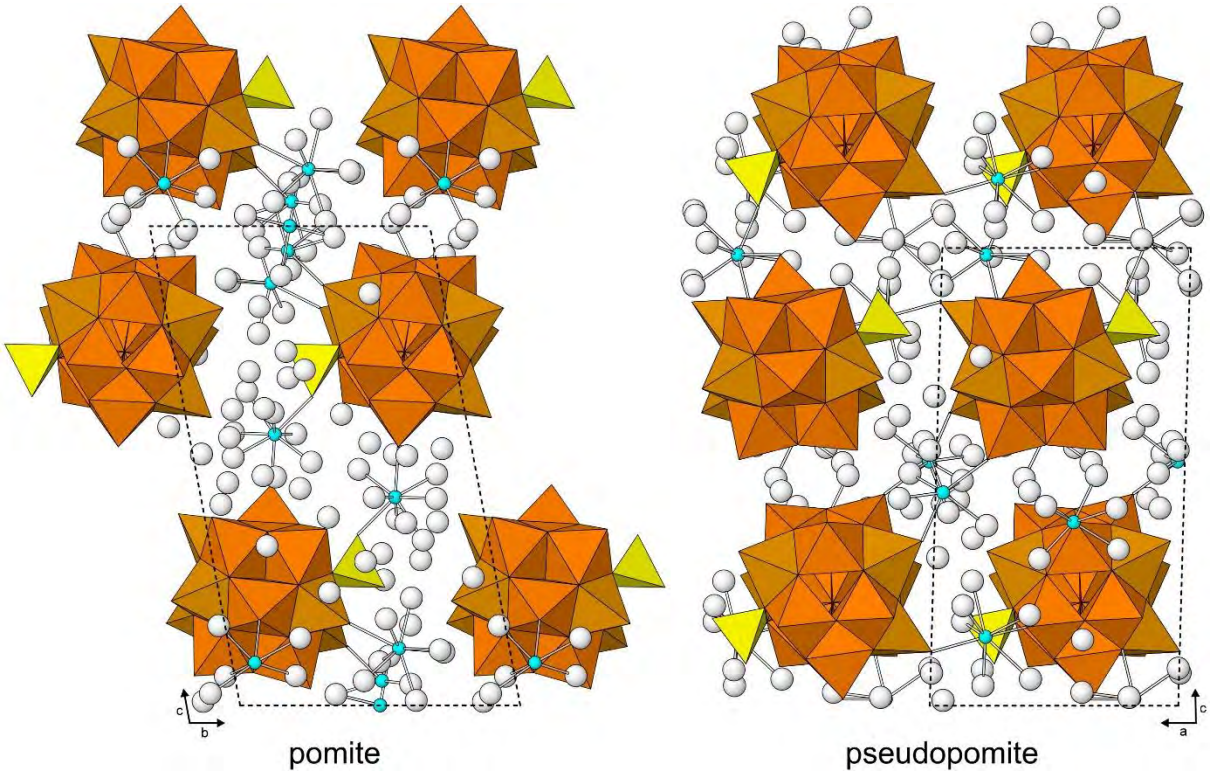

FIGURE 6. The structures of pomite and pseudopomite. The polyhedra are as indicated in Figure 5. The Ca atoms are turquoise balls, the H_2O groups are white balls. The unit cells are outlined with dashed lines. Note that the low-occupancy V15B site in the pomite structure is omitted.

This is the peer-reviewed, final accepted version for American Mineralogist, published by the Mineralogical Society of America.
The published version is subject to change. Cite as Authors (Year) Title. American Mineralogist, in press.
DOI: https://doi.org/10.2138/am-2022-8335. http://www.minsocam.org/

375

376

377 **TABLE 1**. Analytical data (wt%) for pomite and pseudopomite.

378

	Pomite				Pseudopomite				
Oxide	Mean	Range	S.D.	Norm.	Mean	Range	S.D.	Norm.	Standard
CaO	9.05	8.70–9.46	0.24	7.89	9.88	9.73–10.03	0.10	9.42	anorthite
V_2O_5	(70.88)	70.29–71.63	0.45		(68.86)	67.16–70.15	0.96		V metal
VO_2*	22.54			19.65	25.02			23.85	
V_2O_5*	46.17			40.26	41.43			39.48	
CO_2[§]				2.00				2.12	
H_2O[§]				30.20				25.14	
Total				100.00				100.01	

379 * Total V was apportioned between VO_2 and V_2O_5 to attain charge balance.
380 [§] Based upon the crystal structure.
381
382
383

384

385

386

387

This is the peer-reviewed, final accepted version for American Mineralogist, published by the Mineralogical Society of America.
The published version is subject to change. Cite as Authors (Year) Title. American Mineralogist, in press.
DOI: https://doi.org/10.2138/am-2022-8335. http://www.minsocam.org/

388 **TABLE 2.** Selected bond distances (Å) and bond valences (*vu*) in pomite[ξ]

389

Bond	Distance	BV	Bond	Distance	BV	Bond	Distance	BV	Bond	Distance	BV
V1–O12	1.599(11)	1.74	V2–O17	1.627(10)	1.61	V3–O20	1.588(11)	1.79	Ca1–OW1	2.419(11)	0.29
V1–O30	1.713(10)	1.28	V2–O37	1.961(9)	0.65	V3–O25	1.888(11)	0.79	Ca1–OW5	2.443(11)	0.27
V1–O31	1.916(10)	0.74	V2–O38	1.972(10)	0.63	V3–O30	1.913(10)	0.74	Ca1–OW6	2.450(11)	0.27
V1–O26	1.925(10)	0.72	V2–O39	2.005(10)	0.58	V3–O39	1.958(10)	0.66	Ca1–OW2	2.450(11)	0.27
V1–O36	2.034(10)	0.54	V2–O31	2.030(9)	0.54	V3–O6	2.004(10)	0.58	Ca1–O17	2.477(10)	0.25
V1–O2	2.618(12)	0.11	V2–O2	2.329(13)	0.24	V3–O2	2.517(12)	0.15	Ca1–O13	2.508(10)	0.23
<V1–O>	1.968	**5.11**	<V2–O>	1.987	**4.26**	<V3–O>	1.978	**4.71**	Ca1–OW4	2.550(11)	0.21
					3.86			***4.55***	Ca1–OW3	2.595(12)	0.19
									<Ca1–O >	2.487	**1.96**
V4–O13	1.632(10)	1.59	V5–O15	1.609(10)	1.69	V6–O16	1.616(10)	1.66			
V4–O24	1.973(10)	0.63	V5–O35	1.834(10)	0.92	V6–O35	1.820(10)	0.96	Ca2–OW16	2.371(14)	0.32
V4–O28	1.997(10)	0.59	V5–O33	1.916(9)	0.74	V6–O32	1.919(9)	0.73	Ca2–OW10	2.412(15)	0.29
V4–O33	2.012(9)	0.57	V5–O38	1.952(10)	0.67	V6–O37	1.947(9)	0.68	Ca2–OW9	2.466(13)	0.25
V4–O32	2.018(10)	0.56	V5–O34	2.015(9)	0.56	V6–O40	1.994(10)	0.60	Ca2–OW11	2.472(15)	0.25
V4–O1	2.316(13)	0.25	V5–O1	2.643(11)	0.10	V6–O1	2.646(13)	0.10	Ca2–O18	2.490(11)	0.24
<V4–O>	1.991	**4.19**	<V5–O>	1.995	**4.68**	<V6–O>	1.990	**4.72**	Ca2–OW12	2.527(16)	0.22
		3.75			***4.51***			***4.57***	Ca2–OW7	2.534(14)	0.22
									Ca2–OW14	2.542(16)	0.21
V7–O9	1.585(10)	1.80	V8–O10	1.628(10)	1.60	V9–O8	1.626(10)	1.61	<Ca2–O >	2.477	**2.01**
V7–O25	1.964(11)	0.65	V8–O22	1.732(10)	1.21	V9–O22	1.911(10)	0.75			
V7–O26	1.990(10)	0.60	V8–O27	1.918(10)	0.73	V9–O24	1.943(10)	0.68	Ca3–OW25	2.33(2)	0.36
V7–O27	2.023(10)	0.55	V8–O28	1.919(9)	0.73	V9–O23	1.955(11)	0.66	Ca3–OW8	2.386(17)	0.31
V7–O23	2.059(11)	0.50	V8–O29	1.991(9)	0.60	V9–O7	1.993(9)	0.60	Ca3–O4	2.389(11)	0.31
V7–O3	2.216(12)	0.33	V8–O3	2.706(12)	0.09	V9–O3	2.473(12)	0.16	Ca3–OW13	2.405(19)	0.30
<V7–O>	1.973	**4.43**	<V8–O>	1.982	**4.97**	<V9–O>	1.984	**4.47**	Ca3–OW15	2.406(15)	0.30
		4.12			***4.95***			***4.18***	Ca3–O9	2.426(10)	0.28
									Ca3–OW31	2.51(4)	0.23
V10–O11	1.605(11)	1.71	V11–O14	1.617(10)	1.65	V12–O21	1.586(10)	1.80	Ca3–OW35	2.71(4)	0.08
V10–O29	1.905(10)	0.76	V11–O34	1.891(10)	0.79	V12–O34	1.867(10)	0.84	<Ca3–O >	2.445	**2.16**
V10–O26	1.929(10)	0.71	V11–O29	1.912(10)	0.74	V12–O36	1.877(10)	0.82			
V10–O36	1.948(10)	0.68	V11–O28	1.949(9)	0.67	V12–O38	1.909(10)	0.75	Ca4–OW19(×2)	2.18(2)	0.51
V10–O27	1.966(10)	0.64	V11–O33	1.958(9)	0.66	V12–O31	1.952(9)	0.67	Ca4–OW26(×2)	2.38(3)	0.31
<V10–O>	1.871	**4.50**	<V11–O>	1.865	**4.52**	<V12–O>	1.838	**4.88**	Ca4–OW12(×2)	2.810(16)	0.11
		4.23			***4.26***			***4.81***	<Ca4–O >	2.457	**1.88**
V13–O18	1.608(10)	1.69	V14–O19	1.617(11)	1.65	V15A–O5	1.651(12)	1.51			
V13–O37	1.923(10)	0.72	V14–O40	1.903(10)	0.76	V15A–O4	1.659(11)	1.48	Ca5–OW26	2.02(4)	0.76
V13–O40	1.923(10)	0.72	V14–O24	1.931(10)	0.71	V15A–O6	1.784(10)	1.05	Ca5–OW18	2.25(3)	0.43
V13–O39	1.943(9)	0.68	V14–O32	1.942(10)	0.69	V15A–O7	1.792(9)	1.03	Ca5–OW12	2.31(3)	0.37
V13–O6	1.964(10)	0.65	V14–O7	1.984(10)	0.61	<V15A–O>	1.722	**5.07**	Ca5–O19	2.31(3)	0.37
<V13–O>	1.872	**4.47**	<V14–O>	1.875	**4.42**				Ca5–OW11	2.62(3)	0.17
		4.18			***4.11***	V15B–O4	1.552(19)	1.97	Ca5–OW19	2.74(4)	0.13
						V15B–O25	2.002(19)	0.58	Ca5–OW20	2.90(4)	0.09
C–O1	1.244(16)	1.47				V15B–O7	2.050(19)	0.51	<Ca5–O >	2.450	**2.33**
C–O2	1.282(17)	1.34				V15B–O6	2.05(2)	0.51			
C–O3	1.284(17)	1.33				V15B–O23	2.14(2)	0.40			
<C–O>	1.270	**4.14**				<V15B–O>	1.959	**3.98**			
								3.43			

390 [ξ]All V-O bond valences calculated using V^{5+} bond valence parameters of Brown and Altermatt
391 (1985); for V-polyhedra with bond-valence sums <5.0 *vu* in Table 3a, b, the bond-valence of the
392 mixed-valence site is recalculated using the method of Cooper et al. (2019). That revised bond-
393 valence is given in italics below the bond valence calculated with the Brown and Altermatt
394 parameters.
395
396

This is the peer-reviewed, final accepted version for American Mineralogist, published by the Mineralogical Society of America.
The published version is subject to change. Cite as Authors (Year) Title. American Mineralogist, in press.
DOI: https://doi.org/10.2138/am-2022-8335. http://www.minsocam.org/

397 **TABLE 3.** Selected bond distances (in Å) and bond valences (BV in *vu*) in pseudopomite.

Bond	Distance	BV	Bond	Distance	BV	Bond	Distance	BV	Bond	Distance	BV
V1–O12	1.616(16)	1.66	V2–O17	1.615(15)	1.66	V3–O20	1.618(17)	1.65	Ca1–OW4	2.362(18)	0.33
V1–O30	1.734(17)	1.21	V2–O37	1.969(13)	0.64	V3–O25	1.780(16)	1.06	Ca1–OW7	2.426(19)	0.28
V1–O26	1.887(15)	0.80	V2–O38	1.997(15)	0.59	V3–O30	1.922(16)	0.72	Ca1–OW6	2.444(17)	0.27
V1–O31	1.897(15)	0.78	V2–O39	2.005(14)	0.58	V3–O6	1.953(14)	0.67	Ca1–OW3	2.446(18)	0.27
V1–O36	2.063(15)	0.50	V2–O31	2.030(14)	0.54	V3–O39	1.959(14)	0.66	Ca1–O17	2.510(15)	0.23
V1–O2	2.621(17)	0.11	V2–O2	2.318(17)	0.25	V3–O2	2.555(17)	0.13	Ca1–OW8	2.538(18)	0.21
<V1–O>	1.970	**5.04**	<V2–O>	1.989	**4.26**	<V3–O>	1.965	**4.89**	Ca1–O13	2.611(15)	0.18
					3.86			***4.83***	Ca1–OW5	2.642(19)	0.17
									<Ca1–O >	2.497	**1.93**
V4–O13	1.603(14)	1.72	V5–O15	1.608(15)	1.69	V6–O16	1.617(15)	1.65			
V4–O28	1.994(14)	0.60	V5–O35	1.826(16)	0.94	V6–O35	1.835(14)	0.92	Ca2–OW13	2.36(2)	0.33
V4–O24	2.025(13)	0.55	V5–O33	1.924(14)	0.72	V6–O32	1.916(15)	0.74	Ca2–OW15	2.40(3)	0.30
V4–O33	2.036(14)	0.53	V5–O38	1.971(16)	0.64	V6–O37	1.925(14)	0.72	Ca2–OW12	2.40(3)	0.30
V4–O32	2.052(15)	0.51	V5–O34	2.030(16)	0.54	V6–O40	1.968(15)	0.64	Ca2–OW21	2.42(3)	0.29
V4–O1	2.255(16)	0.29	V5–O1	2.633(15)	0.11	V6–O1	2.646(17)	0.10	Ca2–O8	2.452(15)	0.26
<V4–O>	1.994	**4.20**	<V5–O>	1.999	**4.64**	<V6–O>	1.985	**4.77**	Ca2–O11	2.480(15)	0.25
		3.77			***4.44***			***4.64***	Ca2–OW1	2.485(18)	0.24
									Ca2–OW30	2.65(4)	0.16
V7–O9	1.585(15)	1.80	V8–O10	1.611(15)	1.68	V9–O8	1.615(15)	1.66	Ca2–OW23	2.75(4)	0.13
V7–O25	1.933(16)	0.70	V8–O22	1.747(14)	1.16	V9–O22	1.916(13)	0.74	<Ca2–O >	2.489	**2.26**
V7–O26	1.979(14)	0.62	V8–O28	1.911(15)	0.75	V9–O24	1.920(13)	0.73			
V7–O23	2.044(14)	0.52	V8–O27	1.953(14)	0.67	V9–O23	2.005(14)	0.58	Ca3–O4	2.354(18)	0.34
V7–O27	2.083(15)	0.47	V8–O29	1.989(13)	0.60	V9–O7	2.007(14)	0.58	Ca3–O27	2.521(14)	0.22
V7–O3	2.225(14)	0.32	V8–O3	2.657(16)	0.10	V9–O3	2.440(17)	0.18	Ca3–OW10	2.52(2)	0.22
<V7–O>	1.975	**4.44**	<V8–O>	1.978	**4.96**	<V9–O>	1.984	**4.46**	Ca3–OW11	2.53(2)	0.22
		4.14			***4.94***			***4.17***	Ca3–OW2	2.57(2)	0.20
									Ca3–OW20	2.62(4)	0.17
V10–O11	1.649(14)	1.52	V11–O14	1.650(15)	1.51	V12–O21	1.581(18)	1.82	Ca3–OW17	2.67(3)	0.15
V10–O29	1.889(15)	0.79	V11–O34	1.931(16)	0.71	V12–O36	1.831(15)	0.93	Ca3–O9	2.805(18)	0.11
V10–O26	1.941(15)	0.69	V11–O29	1.939(14)	0.69	V12–O34	1.844(15)	0.90	<Ca3–O >	2.574	**1.64**
V10–O36	1.962(16)	0.65	V11–O28	1.956(13)	0.66	V12–O38	1.914(14)	0.74			
V10–O27	1.983(14)	0.61	V11–O33	1.962(14)	0.65	V12–O31	1.948(16)	0.68			
<V10–O>	1.885	**4.26**	<V11–O>	1.888	**4.22**	<V12–O>	1.824	**5.06**	Ca4–OW16	2.19(3)	0.50
		3.86			***3.80***				Ca4–OW19	2.23(4)	0.45
									Ca4–OW25	2.29(5)	0.39
									Ca4–OW28	2.49(4)	0.24
V13–O18	1.595(16)	1.75	V14–O19	1.596(18)	1.75	V15–O5	1.579(17)	1.83	Ca4–O15	2.500(19)	0.23
V13–O37	1.922(14)	0.72	V14–O40	1.904(14)	0.76	V15–O4	1.630(18)	1.60	Ca4–OW25	2.51(4)	0.23
V13–O40	1.927(14)	0.72	V14–O24	1.914(13)	0.74	V15–O7	1.817(15)	0.96	Ca4–O14	2.520(19)	0.22
V13–O6	1.930(14)	0.71	V14–O32	1.930(13)	0.71	V15–O6	1.830(15)	0.93	Ca4–OW14	2.58(4)	0.19
V13–O39	1.966(14)	0.64	V14–O7	1.970(15)	0.64	<V15–O>	1.714	**5.32**	<Ca4–O >	2.414	**2.47**
<V13–O>	1.868	**4.55**	<V14–O>	1.863	**4.60**						
		4.31			***4.38***						
C–O1	1.27(3)	1.34									
C–O2	1.28(3)	1.22									
C–O3	1.32(3)	1.38									
<C–O>	1.29	**3.94**									

398

399

400

401

402 **The Following Tables are for Deposit**

403

404

This is the peer-reviewed, final accepted version for American Mineralogist, published by the Mineralogical Society of America.
The published version is subject to change. Cite as Authors (Year) Title. American Mineralogist, in press.
DOI: https://doi.org/10.2138/am-2022-8335. http://www.minsocam.org/

405

Powder X-ray diffraction data (*d* in Å) for pomite

I_{obs}	d_{obs}	d_{calc}	I_{calc}	*h k l*
		21.578	20	0 0 1
		12.405	47	0 1 0
100	**11.87**	11.918	100	1 0 0
		11.737	69	0-1 1
		11.115	31	-1 0 1
98	**10.62**	10.789	73	0 0 2
30	**10.04**	9.9832	32	0 1 1
		9.9162	5	-1 1 0
		9.8623	5	1 0 1
		9.1197	23	1-1 1
37	**9.06**	9.0109	1	0-1 2
		8.9047	18	-1 1 1
		8.6242	6	-1 0 2
6	7.61	7.6904	2	1 1 0
		7.4916	3	1 0 2
		7.1891	2	-1 1 2
		6.2023	1	0 2 0
		5.9112	1	1-1 3
		5.8683	1	0-2 2
8	5.79	5.8451	1	-2 1 1
		5.7614	1	-1 2 1
		5.6872	2	0 2 1
		5.6320	5	1-2 2
7	5.51	5.5474	6	2 0 1
		5.3944	5	0 0 4
		5.3518	5	-2 1 2
		5.1986	7	0-2 3
14	**5.21**	5.1262	3	-1-2 1
		5.0142	3	1 2 0
		4.9916	2	0 2 2
		4.9611	2	-1-2 2
		4.9428	2	-2 0 3
11	4.92	4.9311	1	2 0 2
		4.9148	1	2 1 0
		4.8313	3	-2-1 2
		4.7218	3	-2 1 3
6	4.69	4.6738	1	1 0 4
		4.6418	3	0 1 4
		4.5882	3	-1-2 3
		4.5599	3	2-2 2
8	4.51	4.5055	1	0-2 4
		4.4879	3	2-1 3
		4.4718	2	-2-1 3
		4.3332	1	0-1 5
		4.3174	1	0 2 3
12	4.30	4.3013	8	2 0 3
		4.2536	2	-1 0 5
		4.2478	1	-1 3 0
		4.1835	1	2 1 2
7	4.14	4.1349	2	0 3 0
		4.1254	2	0-3 2
		4.0909	1	-3 1 0
		4.0822	2	-3 1 1
		4.0424	1	1 1 4
		3.9357	3	-3 1 2
		3.9123	9	-1 1 5
18	**3.921**	3.9078	2	2-1 4
		3.8978	1	0-2 5
		3.8836	1	-2-2 2
		3.8797	1	-2 3 0
		3.8596	1	0 1 5
		3.7587	1	-3 2 1
		3.7458	2	2 0 4
7	3.728	3.7247	1	-2-2 3
		3.7131	1	-1-3 1
		3.7049	1	-3 0 3
		3.6909	2	-3 1 3
		3.5918	2	1-3 4
		3.5533	1	-1-3 3
3	3.477	3.4888	1	-2-2 4
		3.4154	1	1-1 6
		3.3945	1	3 1 1
		3.3406	1	1 2 4
3	3.354	3.3336	1	3-2 3
		3.3164	2	1 0 6
		3.3081	1	0-3 5
		3.3025	1	-2 3 3
		3.2904	1	-2 0 6
5	3.281	3.2828	3	3-3 1
		3.2698	1	1-2 6
		3.2636	1	-1-2 6
		3.2489	1	1 3 2
		3.2331	1	-3-1 4
		3.1553	1	-2 1 6
8	3.161	3.1519	3	-3 0 5
		3.1306	1	0-1 7
		3.1209	1	-2-3 1
		3.1011	1	0 4 0
		3.0915	1	-1 0 7
		3.0886	1	-4 1 1
		3.0833	5	-2 4 0
		3.0763	4	-4 1 0
19	**3.075**	3.0707	1	-3-2 2
		3.0619	1	0-4 3
		3.0590	4	2 3 0
		3.0563	2	2-4 2
		3.0389	3	-4 1 2
		3.0274	2	1 1 6
		3.0210	1	3 2 0
		3.0146	1	2-1 6
11	2.999	3.0094	1	-4 0 1
		3.0036	6	3 0 4
		2.9905	1	0-2 7
		2.9774	2	1 2 5
		2.9702	6	1-1 7
		2.9561	1	2-4 3
		2.9482	2	-1 4 2
		2.9433	1	4-2 1
8	2.937	2.9381	1	-2-3 4
		2.9356	2	-4 1 3
		2.9177	3	-1 1 7
		2.9139	1	3 2 1
		2.9099	1	-2 0 7
		2.8875	2	1 0 7
7	2.895	2.8840	2	4-1 2
		2.8807	1	-2 4 2
		2.8697	2	-1-3 6
		2.8524	1	3-1 5
		2.8346	3	-1 3 5
12	2.826	2.8203	4	-3 1 6
		2.8160	1	2-4 4
		2.8084	1	3-4 1
		2.7934	3	2 3 2
11	2.795	2.7862	4	-2-3 5
		2.7842	1	-4-1 1
		2.7811	1	-3-1 6
		2.7742	3	0-4 5
		2.7706	1	3 2 2
		2.7633	1	3-4 2
		2.7534	1	2-3 6
7	2.755	2.7458	2	-4 3 1
		2.7414	1	4-3 1
		2.7391	1	1 4 1
		2.7265	2	-1-1 8
		2.6845	1	2-1 7
		2.6773	1	1 1 7
		2.6711	1	2 1 6
		2.6530	2	2-4 5
		2.6405	1	-3 2 6
		2.6343	3	-1-3 7
14	**2.632**	2.6203	1	-3 0 7
		2.6182	1	-3-3 2
		2.6145	2	-1-2 8
		2.6076	2	3 2 3
		2.5993	1	0-4 6
		2.5932	1	2 0 7
		2.5863	1	3-2 6
		2.5843	1	-1 4 4
5	2.578	2.5797	1	-2-1 8
		2.5652	1	4-1 4
		2.5635	2	3 3 0
		2.5545	1	1 0 8
		2.5382	1	-2-4 3
		2.5351	1	-2 3 6
		2.5316	1	2-5 2
		2.5256	1	-3-3 4
		2.4972	1	3 0 6
4	2.501	2.4949	1	-1 5 1
		2.4923	1	0-5 3
		2.4727	2	3-3 6
		2.4541	1	-4 4 1
		2.4327	1	2 4 1
4	2.413	2.4143	1	0 5 1
		2.4120	2	5-1 1
		2.4046	1	-1 5 2
		2.3903	1	-2 5 2
		2.3885	2	-3 5 0
		2.3431	1	-1 3 7
		2.3360	2	-1-4 7
		2.3341	1	-4-2 5
2	2.321	2.3259	1	-3-3 6
		2.3221	1	4-3 5
		2.3131	1	2-4 7
		2.2941	1	-2-4 6
		2.2904	1	3-4 6
		2.2714	1	3 3 3
		2.2644	1	3-5 4
		2.2557	1	1 5 1
		2.2272	2	-1 4 6
		2.2069	1	-3-3 7
3	2.197	2.2017	1	-5-1 4
		2.1985	1	-1 -1 10
		2.1801	1	-1 5 4
		2.1760	1	4-5 2
		2.1575	1	-5 4 1
6	2.151	2.1523	1	-1 -2 10
		2.1500	1	5-1 4
		2.1357	1	-4 1 8
		2.1255	1	-5 4 2
		2.1233	1	2 0 9
		2.0751	1	5 0 4
		2.0728	1	1 0 10
5	2.069	2.0640	1	-4 5 3
		2.0622	1	0 1 10
		2.0603	1	-1 5 5
		2.0555	1	-3 6 0
3	2.047	2.0504	1	-1 -3 10
		2.0411	1	-6 2 2
		2.0313	1	-5 1 7
		2.0212	1	2 2 8
		2.0153	1	3-4 8
		2.0122	1	-6 2 3
		1.9966	1	0 5 5
		1.9858	1	3 4 3
		1.9796	1	6-2 2
7	1.971	1.9745	1	4 3 3
		1.9723	1	-4-3 7
		1.9691	1	-1-6 4
		1.9622	2	4-4 7
		1.9566	1	1 6 0
		1.9508	1	-4-4 1
		1.9478	1	-5-2 6
		1.9438	1	6-3 2
		1.9397	1	-5 5 2
		1.9261	1	-2 4 8
		1.9144	1	-1 -4 10
		1.9091	1	-6-1 1
		1.8976	1	-1 -3 11
4	1.910	1.8932	1	-2 1 11
		1.8893	1	6 1 0
		1.8868	1	-5-3 4
		1.8556	1	-5 4 6
		1.8440	1	2 -2 11
		1.8294	1	-3 1 11
		1.8171	1	-3 -2 11
		1.8118	1	6 1 2
		1.8021	1	4 3 5
		1.8000	1	0-7 3
		1.7973	1	-4 4 8
		1.7914	1	-1 4 9
		1.7849	1	-5 6 1
		1.7464	1	1 -3 12
		1.7355	1	2 2 10
		1.7329	1	0-6 9
		1.7140	1	-5 5 6
		1.7076	1	1 3 10
		1.7066	1	4-6 7
		1.6973	1	6 2 2
		1.6923	1	3 3 8
		1.6909	1	4-7 4
		1.6707	1	1 4 9
		1.6693	1	7-4 1
		1.6668	1	6-4 6

406

407

408

Powder X-ray diffraction data (*d* in Å) for pseudopomite

I_{obs}	d_{obs}	d_{calc}	I_{calc}	*h k l*
		11.1270	50	0 1 0
100	**10.94**	11.0772	80	1 0 0
		10.7601	100	0 1 1
		10.3854	3	1 1 0
		10.2020	78	0 0 2
73	**10.00**	9.9629	74	1 1 1
		9.8491	25	-1 0 1
		9.6250	10	1 0 1
31	**8.86**	9.0092	22	0-1 1
		8.6801	22	-1-1 1
		8.4511	2	0 1 2
		7.9855	3	1 1 2
		7.6090	4	-1 0 2
5	7.51	7.4037	14	1 0 2
		6.4323	4	0 1 3
4	6.13	6.1907	4	1 1 3
		5.9964	5	2 1 1
4	5.71	5.7264	3	1 0 3
		5.6772	6	0 2 1
		5.5635	2	0 2 0
		5.5386	3	2 0 0
16	**5.32**	5.3800	11	0 2 2
		5.3085	10	2 0 1
		5.1927	4	2 2 0
9	5.08	5.1010	15	0 0 4
		5.0581	2	-2-1 2
		4.9814	2	2 2 2
7	4.82	4.9202	5	1 1 4
		4.8204	5	-1-2 2
		4.8125	2	2 0 2
		4.6824	4	-1 0 4
		4.5858	2	1 0 4
		4.5124	4	2 2 3
11	**4.42**	4.4187	14	1 2 4
		4.3400	3	-2-2 2
8	4.26	4.3083	6	0-1 4
		4.2888	2	-1 2 0
		4.2802	2	-2 1 0
		4.2381	3	2 0 3
		4.2256	5	0 2 4
		4.1850	3	1 3 1
		4.0983	2	-2 1 2
9	4.082	4.0833	2	1 3 0
		4.0636	3	3 1 0
		4.0514	5	2 3 1
		3.9552	2	3 2 0
6	3.835	3.8444	10	-1-3 1
		3.8008	4	-2 1 3
		3.7961	4	1 2 5
		3.5959	8	0-1 5
3	3.540	3.5615	2	3 1 3
		3.5479	2	-3-2 2
		3.4615	4	3 3 2
		3.4007	2	0 0 6
		3.3516	2	0 3 4
		3.2840	6	-2 2 0
3	3.272	3.2687	2	-2-1 5
		3.2524	2	3 1 4
		3.2084	3	-1 1 6
		3.2035	2	-1-3 3
		3.1877	3	2 3 5
		3.1658	2	-1 3 2
10	3.145	3.1336	2	-2 2 3
		3.1306	6	2 4 2
		3.1092	2	-3-1 4
		3.0954	2	2 2 6
		3.0846	2	2 1 6
		3.0773	7	0-1 6
22	**3.074**	3.0687	5	2 4 0
		3.0606	3	4 2 1
		3.0562	4	4 2 0
		3.0308	3	-3 0 4
		3.0178	2	1 4 3
		3.0046	7	0-2 5
		2.9764	4	0 1 7
		2.9555	7	-2 2 4
19	**2.953**	2.9520	6	1 3 6
		2.9428	2	-2-4 1
		2.9389	4	1 1 7
		2.9341	3	-2 0 6
		2.9231	7	3-1 2
		2.9176	2	4 3 1
18	**2.890**	2.8923	7	-1-3 4
		2.8852	3	4 3 2
		2.8619	4	-4-2 2
		2.8170	4	0 3 6
		2.8141	3	2-1 5
		2.8107	3	-4-3 1
		2.7870	2	0 4 3
		2.7772	4	4 1 3
11	2.773	2.7397	4	0-3 4
		2.7252	5	4 2 4
		2.7229	2	-4-1 3
		2.6913	2	-4 0 2
		2.6406	2	-2 3 1
		2.6247	2	4 4 2
6	2.602	2.6132	3	-1-3 5
		2.6080	2	-2 3 0
		2.5802	3	1 1 8
		2.5587	3	1 2 8
		2.5508	4	2 0 7
		2.5467	2	-2 2 6
7	2.537	2.5406	2	4 0 3
		2.5365	3	2-3 1
		2.5245	3	4 3 5
		2.5226	3	-4-4 1
		2.4967	2	2 5 3
		2.4891	2	-2 3 4
4	2.472	2.4623	2	-4 0 4
		2.4558	2	3-2 2
		2.4361	2	2 5 4
3	2.383	2.3901	4	-4-1 5
		2.3648	2	-5-3 1
		2.3471	2	4-1 2
5	2.209	2.2231	2	-4-1 6
		2.2131	2	3-1 6
4	2.159	2.1518	2	4-1 4
5	2.097	2.0868	3	-1 4 7
8	2.050	2.0404	2	0 0 10
5	1.988	1.9969	2	1 0 10
		1.9719	2	6 2 3
5	1.944	1.9421	2	-3-1 9
5	1.828	1.8202	2	-1 2 11
		1.7865	2	5 6 6
		1.7437	2	-1 3 11
		1.7096	2	4 1 10

409

410